International Journal on Magnetic Particle Imaging
Vol 8, No 1, Suppl 1, Article ID 2203023, 4 Pages

Infinite Science Publishing

Proceedings Article

Side Lobe Informed Center Extraction (SLICE): a projection-space forward model reconstruction for a 2D imaging system

Erica E. Mason [a,*] · Stephen F. Cauley [a] · Eli Mattingly [a,b,c] · Monika Śliwiak [a] · Lawrence L. Wald [a,c]

[a] Martinos Center for Biomedical Imaging, Massachusetts General Hospital, Charlestown, MA, USA
[b] Massachusetts Institute of Technology, Cambridge, MA, USA
[c] Harvard Medical School, Boston, MA, USA
[*] Corresponding author, email: emason1@mgh.harvard.edu

Abstract

A two-dimensional MPI acquisition allows signal from superparamagnetic iron oxide nanoparticles (SPIONs) outside the intended 2D imaging plane to interfere destructively with that from SPIONs in the desired slice, creating unwanted artifacts in the reconstructed image. We address this "side-lobe" signal interference with a Side Lobe Informed Center Extraction (SLICE) reconstruction, which utilizes a projection-space 3D forward model of the detected harmonics. The developed method reduces the out-of-plane interference artifacts in the 2D image reconstruction without the need to change the simplified acquisition schemes or hardware of the gradiometer detection based field-free line system, for example by adding true 3D encoding which would interfere with the goal of fast <5 second temporal resolution needed for functional brain imaging.

I. Introduction

Our projection-based MPI field-free line (FFL) imager for rodent functional brain imaging (details on OS-mpi.github.io [1]) was designed as a 2D imager with <5 sec temporal resolution to resolve hemodynamic changes during brain activation. The imager utilizes a permanent magnet FFL and electromagnet shift coils that rotate about z to acquire projections in the $x-y$ plane. Superparamagnetic iron oxide nanoparticle (SPION) magnetization is driven at $f_0 = 25$ kHz by a solenoidal drive coil in the z direction and detected with a separate z directed solenoid in a gradiometer configuration. With a drive amplitude of ∼10 mT peak, this sweeps the 2.8 T/m gradient FFL in z over a ∼7.2 mm pk-pk distance. In this configuration, the achievable point spread function (PSF) along z contains significant contribution from out-of-slice SPIONs, as seen in the simulated harmonic sensitivity profiles (Fig. 1). Since the receive (Rx) coil detects the integrated SPION magnetization in its sensitive volume, signal from outside the imaging slice will interfere (destructively if opposite phase) with in-plane signal unless accounted for. When imaging brain blood volume changes in rodents, SPION signal from large vessels outside the imaging slice, for instance, can be observed in the 2D image reconstruction. Here, we present a forward model reconstruction to suppress signal interference from out-of-slice SPIONs in the 3rd dimension.

X-space MPI and System Matrix MPI both enable 3D acquisition and reconstruction with great success [2, 3]. Implementing such approaches in our 2D projection

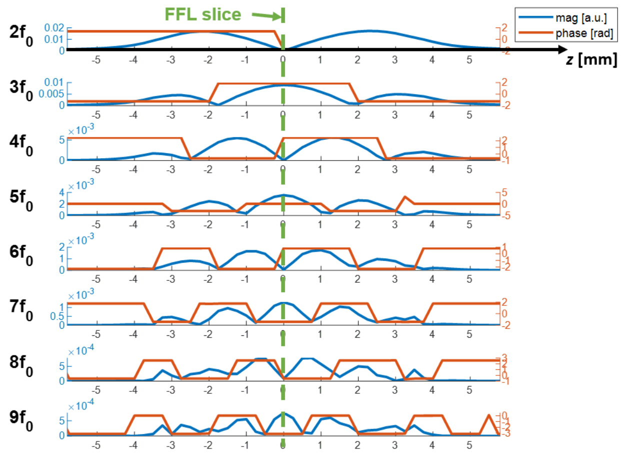

Figure 1: Simulated sensitivity profiles along the center of the bore, $(0,0,z)$ formed by calculating signal induced by a SPION point source of Synomag®-D 70 nm placed at each location along z for $2f_0$-$9f_0$. Magnitude = blue, phase = orange.

scanner, as done traditionally, would, however, require significant changes to our current acquisition scheme and/or hardware. This would involve either increased scan times to acquire volume data (by either moving the animal or using slice-selecting shift coils), or moving away from a permanent magnet-based mechanically-rotated FFL system.

We formulate a reconstruction more amenable to our existing infrastructure: a projection-space 3D forward model reconstruction with the goal of accounting for signal from SPIONs present in the out-of-plane sensitive regions ("side lobes") and preventing this signal from aliasing into the imaging slice: "Side Lobe Informed Center Extraction" (SLICE). The forward model of our imaging system predicts the complex-valued projections of the first 8 harmonics over a 3D volume. To form a projection from each harmonic's signal level, we bucket the time domain data for each projection sweep into n_p projection points, Fourier transform each bucket of data, and then map the narrow-band signal at each of the n_h harmonics to its point along the projection (i.e. location of the FFL), thereby forming 2D projections of each harmonic. The drive field's movement of the FFL in the z direction is encoded by the differing sensitivity profiles in z of the projections at the higher frequencies. The SPION concentration at the imaging slice ($z = 0$) is determined through inversion of the linear forward model.

II. Methods and materials

The SLICE reconstruction solves the linear system of equations $Ax = b$, where A is the complex-valued forward model in projection space over a 3D volume, and b is the complex 2D projection data acquired with the imager at the n_h harmonics. The forward model is implemented in MATLAB (MathWorks, Natick, MA) utilizing field maps (for drive, receive, shift coils and FFL permanent magnets) produced via Biot-Savart calculations, FEMM 4.2 [4], and Ansys Maxwell (Ansys Inc., Canonsburg, PA). The Langevin model comes from SPION magnetization data measured with an MPS system [1]. The simulated signal is scaled by a measured transfer function of the receive chain. The calculation of induced voltage follows previous work [5]. Fig. 2 shows the structure of the system of equations. The forward model is built by simulating the n_h harmonic projections (each with n_p projection points and n_θ angles used in the image acquisition) for a SPION point source moved to each location in the $n_{pixels} \times n_z$ volume. The normal system of equations is solved with the preconditioned conjugate gradients method. The reconstruction is the real, positive portion of the solution at the center ($z = 0$) slice.

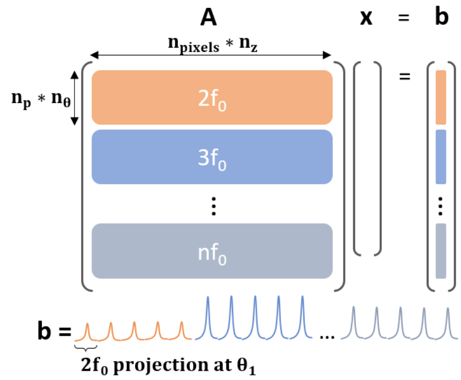

Figure 2: Structure of the system of equations. The forward model (A) has size $[n_p \cdot n_\theta \cdot n_h] \times [n_{pixels} \cdot n_z]$, where n_p, n_θ, n_h, n_{pixels}, and n_z denote numbers of: points per projection, projection angles, harmonics, pixels in the 2D image, and z slices in the model, respectively. A is formed by simulating the projection data induced by a point source at each voxel location of the 3D volume and appending the projections at the harmonics row-wise.

We image a 17 mm inner diam. sphere filled with 31.25 μg/ml Synomag®-D PEG 25.000-OMe 70 nm (micromod, Germany). We image the sphere at multiple locations along the bore with a 5 sec acquisition (66 points per projection, 27 projections covering 180°, $2f_0$-$9f_0$ frequencies acquired). We reconstruct the acquired 2D data using the $[2f_0, 3f_0]$ projections. The SLICE 3D model covers [3 cm × 3 cm × 7.6 mm] discretized into [65 × 65 × 9] locations. The preconditioned conjugate gradients is run for 50 iterations. To compare the SLICE image to a 2D reconstruction, which clearly exhibits interference artifacts from out-of-plane SPIONs, we also reconstruct the data ($3f_0$ magnitude projections) via the inverse radon transform.

10.18416/ijmpi.2022.2203023

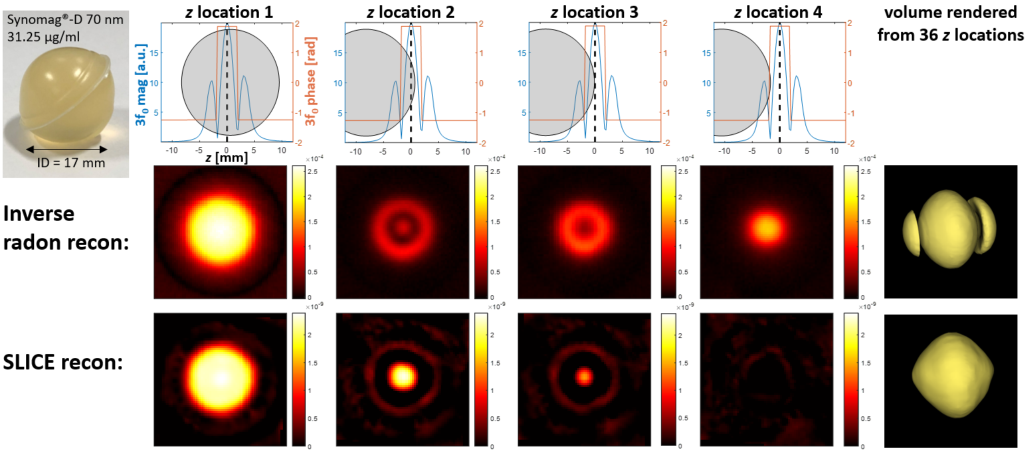

Figure 3: Spherical 17 mm inner diam., 31.25 μg/ml Synomag®-D 70 nm phantom imaged at different z locations along bore and reconstruction of data for each acquisition with the inverse radon reconstruction (second row), and the SLICE recon (third row). Each column indicates a different phantom placement along z, as illustrated in the top row, where the sphere outline is overlaid onto the $3f_0$ sensitivity profile (magnitude = blue, phase = orange). The imaging slice is $z = 0$ (dashed line). The inverse radon transform demonstrates the signal interference from out-of-slice SPIONs. The final column shows a volume rendering formed by stacking the reconstructed images for 36 locations along the bore, made with InVesalius 3 software (github.com/invesalius/).

III. Results

As shown in Fig. 3, the 2D inverse radon reconstructions are contaminated by the interfering signal in the measured projections from out-of-slice SPIONs, with signal appearing even for the sphere placed fully outside of the imaging plane (z locations 3, 4). We see that the interference artifacts are significantly reduced using the SLICE reconstruction. Only the center (FFL plane) solution is utilized; interfering signal from out of slice is correctly restricted from the 2D reconstruction.

IV. Discussion and conclusions

We present the SLICE reconstruction method to address the problem of 3D object interference in a 2D encoded MPI acquisition, utilizing projections at additional harmonics of the drive frequency and a simulated forward model that coarsely represents the system in the third dimension. The harmonic projection data from a 2D encoded FFL scanner can be reconstructed with an improved "slice" PSF compared to fully 2D reconstructions. Although this "3D reconstruction" is not currently used to form a full 3D image in a single acquisition, it informs the reconstruction's removal of signal from out of slice. Thus, the reconstruction method we present here helps to enable fast (5 sec) 2D projection reconstruction imaging with reduced interference artifacts, with no change in the hardware or data acquisition times.

Additional encoding information could be provided by added Rx coils receiving signal in x and/or y to acquire the transverse magnetization data [6]. Similar to many System Matrix MPI reconstruction methods, the forward model can also be measured [3]. While time consuming, this calibration procedure could produce a more accurate forward model. Further work is underway to improve the reconstruction algorithm, including penalizing solutions which are not real/positive, utilizing additional harmonics, adding regularization, and allowing for a phase offset term in the model.

Acknowledgments

We thank Jochen Franke for first alerting us to the expectation of side lobes in the z PSF of our 2D imager. We thank Martin Hürlimann for insightful discussion and ideas, and we thank Konstantin Herb, John Drago and Alex Barksdale for helpful conversations. Research funding: NIBIB U01EB025121.

Author's statement

Conflict of interest: Authors state no conflict of interest.

References

[1] E. Mattingly, E. E. Mason, K. Herb, M. Śliwiak, K. Brandt, C. Z. Cooley, and L. L. Wald. OS-MPI: An open-source magnetic particle imaging project. *Int. J. Magn. Part. Imaging*, 6(2):1–3, 2020, doi:10.18416/IJMPI.2020.2009059.

[2] P. W. Goodwill, J. J. Konkle, B. Zheng, E. U. Saritas, and S. M. Conolly. Projection x-space magnetic particle imaging. *IEEE Trans. Med. Imaging*, 31(5):1076–1085, 2012.

[3] J. Weizenecker, B. Gleich, J. Rahmer, H. Dahnke, and J. Borgert. Three-dimensional real-time in vivo magnetic particle imaging. *Phys. Med. Biol.*, 54:L1–L10, 2009, doi:10.1088/0031-9155/54/5/L01.

[4] D. C. Meeker, Finite Element Method Magnetics, Version 4.2 (21Apr2019 Build), [Online]. Available: https://www.femm.info.

[5] E. E. Mason, C. Z. Cooley, S. F. Cauley, M. A. Griswold, S. M. Conolly, and L. L. Wald. Design analysis of an MPI human functional brain scanner. *Int. J. Magn. Part. Imaging*, 3(1), 2017, doi:10.18416/ijmpi.2017.1703008.

[6] P. Goodwill and S. Conolly. Multidimensional x-space magnetic particle imaging. *IEEE Trans. Med. Imaging*, 30(9):1581–1590, 2011.

10.18416/ijmpi.2022.2203023